

## Field-Induced Order-Disorder Transition in Antiferromagnetic $\text{BaCo}_2\text{V}_2\text{O}_8$ Driven by a Softening of Spinon Excitation

S. Kimura,<sup>1</sup> H. Yashiro,<sup>1</sup> K. Okunishi,<sup>2</sup> M. Hagiwara,<sup>1</sup> Z. He,<sup>3</sup> K. Kindo,<sup>3</sup> T. Taniyama,<sup>4</sup> and M. Itoh<sup>4</sup>

<sup>1</sup>*KYOKUGEN, Osaka University, Machikaneyama 1-3, Toyonaka 560-8531, Japan*

<sup>2</sup>*Department of Physics, Niigata University, Niigata 950-2181, Japan*

<sup>3</sup>*Institute for Solid State Physics, University of Tokyo, Kashiwa 277-8531, Japan*

<sup>4</sup>*Materials and Structures Laboratory, Tokyo Institute of Technology, 4259 Nagatsuta, Midori Yokohama 226-8503, Japan*

(Received 16 April 2007; published 24 August 2007)

High field magnetization and ESR measurements on the quasi-one-dimensional (1D) antiferromagnet  $\text{BaCo}_2\text{V}_2\text{O}_8$  have been performed in magnetic fields up to 50 T along the chain. The experimental results are explained well in terms of a 1D  $S = 1/2$  antiferromagnetic XXZ model in longitudinal fields. We show that the quantum phase transition from the Néel ordered phase to the spin liquid one in the model is responsible for a peculiar order to disorder transition in  $\text{BaCo}_2\text{V}_2\text{O}_8$ .

DOI: [10.1103/PhysRevLett.99.087602](https://doi.org/10.1103/PhysRevLett.99.087602)

PACS numbers: 76.50.+g, 75.10.Pq, 75.50.Ee

Quantum phase transitions (QPTs) are very unconventional phenomena, caused by quantum fluctuations near absolute zero Kelvin. The most promising objects to explore the QPTs are quantum spin systems in magnetic fields. Field-induced magnetic order in the spin gap systems, which was demonstrated as a realization of the Bose-Einstein condensation of magnon quasiparticles, is an example of intense study [1,2]. In contrast to this field-induced order, another peculiar phenomenon, in which the long range order is destroyed in the presence of applied magnetic fields, was recently found in the quasi-one-dimensional (1D) antiferromagnet  $\text{BaCo}_2\text{V}_2\text{O}_8$  [3]. In this Letter, this field-induced order to disorder transition is revealed to be a novel type of the QPT. We show that the QPT from the Néel ordered phase to the spin liquid one in a 1D  $S = 1/2$  antiferromagnetic XXZ model in longitudinal fields is responsible for the order to disorder transition in  $\text{BaCo}_2\text{V}_2\text{O}_8$ .

$\text{BaCo}_2\text{V}_2\text{O}_8$  is a quasi-1D  $\text{Co}^{2+}$  spin system, in which edge-shared  $\text{CoO}_6$  octahedra form a screw-chain structure along the  $c$  axis [4]. Owing to an inevitable interchain interaction, this compound undergoes long range ordering at 5.4 K at zero magnetic field [3]. The recent study by He *et al.* revealed the field-induced order to disorder transition in  $\text{BaCo}_2\text{V}_2\text{O}_8$  [3]. When the external field is applied to the  $c$  axis, which is the easy axis of  $\text{BaCo}_2\text{V}_2\text{O}_8$ , the magnetization curve at 2 K exhibits a steep increase above  $H_c \approx 4$  T. The heat capacity measurements showed that the magnetic ordering temperature is rapidly lowered by the external field for  $H \parallel c$ , and in the field region above  $H_c$  no magnetic ordering is observed down to 1.8 K.

In this Letter the results of high field magnetization and high frequency ESR measurements on  $\text{BaCo}_2\text{V}_2\text{O}_8$  in magnetic fields up to 50 T are reported. A 1D model is adopted for quantitative analyses of the experimental results, and interchain interactions are mostly not taken into account. We show that the magnetization curve for  $H \parallel c$  up to the saturation magnetization is reasonably explained

by the 1D  $S = 1/2$  antiferromagnetic XXZ model with Ising-like interaction of  $\epsilon \approx 0.5$  in longitudinal fields. The model is given by the Hamiltonian

$$\mathcal{H} = J \sum_i \{S_{i,z}S_{i+1,z} + \epsilon(S_{i,x}S_{i+1,x} + S_{i,y}S_{i+1,y})\} - g\mu_B \sum_i S_{i,z}H, \quad (1)$$

where  $J > 0$  is the antiferromagnetic exchange interaction and  $\epsilon$  is an anisotropic parameter. A fluctuation mode characteristic of this model is the domain wall pair excitation [5], i.e., spinon, which can be studied by the high frequency ESR in very high accuracy. The ESR measurements indicate that destruction of the long range magnetic order of  $\text{BaCo}_2\text{V}_2\text{O}_8$  is caused by the softening of the spinon excitation at  $H_c$ . The quenching of the spinon excitation gap brings about the transition to the gapless spin liquid phase with no order. Furthermore, the ESR modes suggest a development of soft modes at incommensurate wave vector above  $H_c$ , which is believed as a general feature of gapless 1D quantum antiferromagnets with no classical counterpart.

The high field magnetization of  $\text{BaCo}_2\text{V}_2\text{O}_8$  for  $H \parallel c$  was measured at 1.3 K in pulsed magnetic fields. The ESR measurements in the frequency region up to 2 THz were conducted in pulsed fields up to 50 T at 1.3 K. Detailed frequency dependence of the ESR spectrum below 616 GHz in static magnetic field up to 14 T at 1.6 K was measured by utilizing a vector network analyzer and a superconducting magnet.

As shown in Fig. 1, the high field magnetization curve of  $\text{BaCo}_2\text{V}_2\text{O}_8$  for  $H \parallel c$  at 1.3 K indicates a sharp transition at  $H_c = 3.9$  T. Above  $H_c$ , the magnetization exhibits a nonlinear increase, suggesting the strong quantum fluctuation for  $H > H_c$ , and then shows a transition to the field-induced ferromagnetic phase at  $H_s = 22.7$  T, accompanied by a peak of field derivative of the magnetization ( $dM/dH$ ). The magnetization shows a linear increase

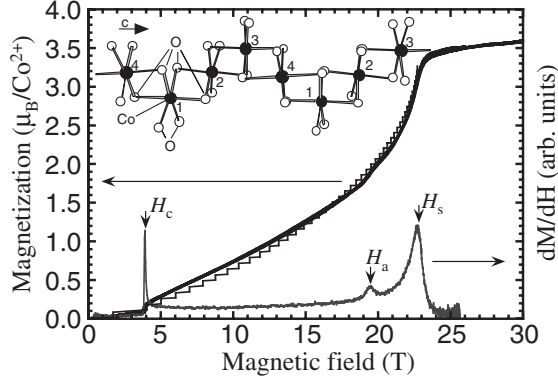


FIG. 1. High field magnetization of  $\text{BaCo}_2\text{V}_2\text{O}_8$ , observed for  $H \parallel c$  at 1.3 K. Bold and thin lines show the experimental and the calculated results, respectively. Gray lines show the field derivative of the magnetization. Inset shows the four-step screw chain of  $\text{BaCo}_2\text{V}_2\text{O}_8$ .

even in the field region above  $H_s$ . We attribute this linear magnetization to the Van Vleck paramagnetic contribution, which gives a magnetic susceptibility with no field dependence. Since the slope of the magnetization curve below  $H_c$  is almost identical to that above  $H_s$ , we conclude that the finite magnetization below  $H_c$  is also due to the Van Vleck paramagnetism. The similar magnetization curve was observed in the Ising-like  $\text{Co}^{2+}$  spin system  $\text{CsCoCl}_3$  for its easy axis [6], and the magnetization curve of  $\text{CsCoCl}_3$  was explained by the  $S = 1/2$  1D XXZ model in the longitudinal field, taking the intrachain ferromagnetic next-nearest-neighbor (NNN) interaction  $J'$  into account [7]. We analyze the magnetization curve of  $\text{BaCo}_2\text{V}_2\text{O}_8$  in terms of the same model. Figure 1 shows that the magnetization curve is explained well by the density matrix renormalization group calculation for a 96-site system with the parameters of  $g = 6.2$ ,  $J/k_B = 62.5$  K,  $\epsilon = 0.53$ ,  $J'/J = -0.065$ , and  $\epsilon' = 0.8$ , where  $\epsilon'$  is an anisotropic parameter of the NNN interaction. The first magnetization step, seen in the theoretical curve at 1.8 T, is merely due to size effect and should be ignored. The Van Vleck paramagnetic contributions, given by the field-independent susceptibility  $\chi_{\text{VV}} = 0.013 \mu_B/T$ , is added to the above calculated magnetization. As previously reported in our brief report, the similar calculated result can be obtained from the exact solution of the  $S = 1/2$  XXZ model with  $J/k_B = 65$  K,  $\epsilon = 0.46$ , and no NNN interaction [8]. However, the NNN interaction is required for quantitative agreements with the results of the ESR measurements. A small anomaly is seen in the  $dM/dH$  curve at  $H_a = 19.5$  T, where the magnetization, subtracting the Van Vleck contribution, approaches to half of its saturation value. We consider that this behavior relates to a four-step periodical structure of Co-O chain in  $\text{BaCo}_2\text{V}_2\text{O}_8$ , that will be mentioned later.

It is known that the low temperature magnetic state of  $\text{Co}^{2+}$  ion in an octahedral ligand field is described by a highly anisotropic effective spin  $S = 1/2$ . This is because the orbital degeneracy of  $\text{Co}^{2+}$  is not lifted by the cubic

crystal field, and the lowest Kramer's doublet, which can be regarded as the effective  $S = 1/2$ , results from the level splitting due to the symmetry lowering and the spin-orbit coupling [9,10]. Furthermore, the recent theory showed that the effective ferromagnetic NNN interaction is derived from the second order perturbation process via crystal-field excited states of  $\text{Co}^{2+}$  ion [7].  $\delta/\lambda = 2.0$ , where  $\delta$  is the strength of the tetragonal distortion and  $\lambda$  is the spin-orbit coupling constant, gives the calculated values  $g = 5.7$  and  $\epsilon = 0.49$  [9,10], which agree fairly well with the experimental ones. The theory of Shiba *et al.* gives  $J'/J \approx -0.075$  and  $\chi_{\text{VV}} \approx 0.01$  for  $\delta/\lambda = 2.0$  [7], which also agree with the experimental values. The anisotropic parameter  $\epsilon < 1$ , indicates the Ising-like interaction in  $\text{BaCo}_2\text{V}_2\text{O}_8$ , as well as  $\text{CsCoCl}_3$ . In the ground state of the  $S = 1/2$  1D XXZ model with  $\epsilon < 1$ , a Néel order is known to exist at zero field [11,12]. When the longitudinal field is applied, however, it was theoretically demonstrated that the spin state between  $H_c$  and  $H_s$  turns into gapless spin liquid similar to the  $S = 1/2$  1D isotropic Heisenberg antiferromagnet [13,14]. Thus, Shiba *et al.* previously predicted that the spin liquid state with no long range order appears in the field-induced phase of  $\text{CsCoCl}_3$  [7]. The prediction has not been confirmed experimentally in  $\text{CsCoCl}_3$ , because of its rather high critical field  $H_c = 33$  T. We consider that this theoretically predicted spin liquid state is realized in  $\text{BaCo}_2\text{V}_2\text{O}_8$ . Our ESR measurements support the realization of the spin liquid state above  $H_c$  and indicate a key role of the spinon excitation for driving the field-induced transition, as will be described below.

Figures 2(a) and 2(b) show the ESR spectra of  $\text{BaCo}_2\text{V}_2\text{O}_8$  for  $H \parallel c$ , observed in static fields at frequencies below 616 GHz at 1.6 K, and those in pulsed fields at 1.3 K, respectively. In the field region below  $H_c$ , a number of ESR signals are observed. The frequency-field diagram of the ESR signals is shown in Fig. 3. The obtained ESR modes exhibit linear field dependences with  $g \approx \pm 6$  below 3 T, showing similar behavior with  $\text{CsCoCl}_3$  [7]. As shown in the inset of Fig. 3, however, the lowest  $A_{-1}$  mode, observed at frequencies below 400 GHz, deviates from the linear dependence above 3 T and shows an approach to zero at  $H_c$ . The ESR modes in  $\text{CsCoCl}_3$  were explained by a theory of Shiba as follows [7,15]. The low-lying excitation of the  $S = 1/2$  1D XXZ model for  $\epsilon < 1$  is the spinon, that is a pair of quantum domain walls propagating through the chain [5]. The excitation spectrum of the spinon forms a continuum with total magnetic quantum numbers  $S_z = \pm 1$ , and has an excitation gap at zero magnetic field. The theory demonstrates that when the three-dimensional ordered state is realized owing to the inevitable interchain interaction, molecular fields, coming from the interchain interaction, quantize the excitation continuum into discrete levels [15]. In finite magnetic fields, each level splits into two branches with  $S_z = +1$  or  $-1$ , giving rise to a number of linear ESR modes. Distributions of the ESR modes in wide frequency region over 3 THz are

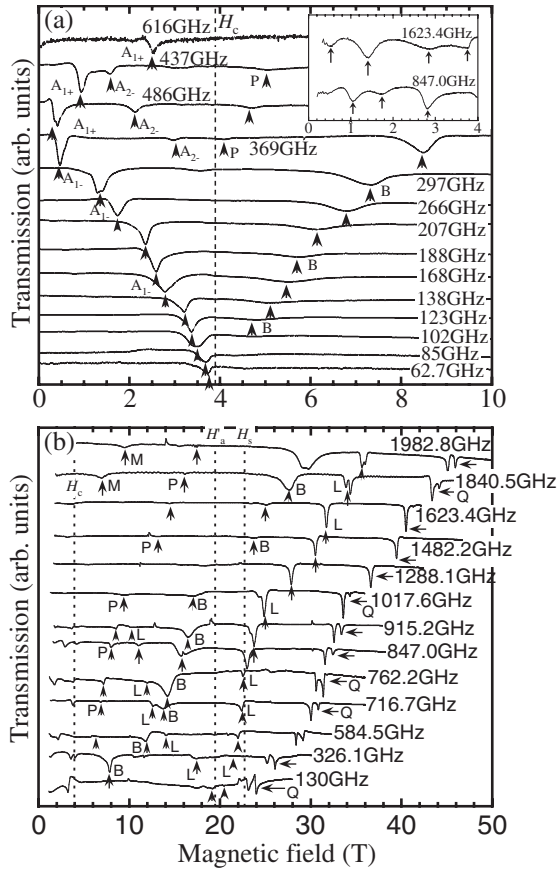


FIG. 2. (a) Frequency dependence of the ESR spectra observed in static magnetic fields below 616 GHz. The inset shows the low-field ESR spectra observed in pulsed fields at 847.0 and 1623.4 GHz. (b) Frequency dependence of the ESR spectra in pulsed fields. Dotted lines show  $H_c$ ,  $H_a$ , and  $H_s$ .

expected from the theoretical calculation with the parameters  $J/k_B = 62.5$  K and  $\epsilon = 0.53$ . The nonlinear dependence of the ESR mode is attributed to a reduction of the interchain molecular field near  $H_c$ . While energies of the quantized levels depend on a strength of the interchain molecular field [15], fluctuation of the ordered moments due to the quantum effect reduces the molecular field. When the external field approaches  $H_c$ , the fluctuation is enhanced as the spinon excitation gap decreases. Therefore, the molecular fields diminish with increasing the external field, giving rise to the nonlinear field dependence. This result suggests that the analysis in terms of the 1D model with no interchain interaction is reasonable for the field region above  $H_c$ .

A significant role of the spinon excitation for a zero-field QPT of the  $S = 1/2$  1D XXZ model was suggested by a theory of Gómez-Santos [12]. At zero magnetic field, as the anisotropic parameter  $\epsilon$  is increased from zero, a QPT from the Néel ordered to the spin liquid phase is known to take place at the Heisenberg point  $\epsilon = 1$  [11, 12]. Gómez-Santos theoretically indicated that the destruction of the Néel order appears as a consequence of a vanishing of the energy necessary for a creation of a spinon at  $\epsilon = 1$  [12].

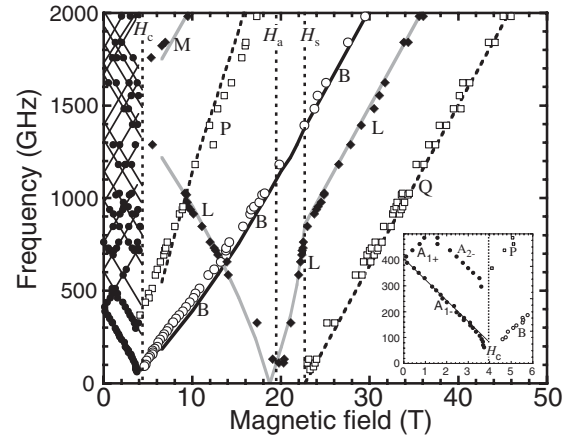


FIG. 3. Frequency-field relation of the ESR resonance points. Symbols represent the ESR resonance points in  $\text{BaCo}_2\text{V}_2\text{O}_8$ . Bold black curves, gray curves, and dashed curves show theoretical excitation energies at  $q = 0$ ,  $\pi/2$ , and  $\pi$ , respectively. Thin solid lines are guides for the eye. Dotted vertical lines show  $H_c$ ,  $H_a$ , and  $H_s$ . The inset shows the extended figure below 500 GHz.

The observed  $A_{1-}$  mode indicates that for the field-induced order to disorder transition in  $\text{BaCo}_2\text{V}_2\text{O}_8$  a softening of the spinon excitation also occurs at the critical point  $H_c$ , and propagation of the domain wall pair destroys the long range order for  $H > H_c$ .

Next we discuss the ESR modes in the field-induced phase above  $H_c$ . Several numbers of new ESR modes appear for  $H > H_c$ . The  $B$  mode with the strongest signal intensity, which shows a positive field dependence, indicates a reopening of the excitation gap at  $q = 0$  above  $H_c$ . The resonance frequency of the  $L$  mode decreases with increasing the field and closes to zero at  $H_a$ . Then, it increases as the field is increased above  $H_a$ . Above the saturation field  $H_s$ , the ESR modes  $Q$ , consisting of two peaks, start to appear. Splitting of these two peaks, which is about 1 T, are much larger than the maximum splitting of the ESR signals expected for the Walker modes, which is estimated to be several hundred millitesla for  $\text{BaCo}_2\text{V}_2\text{O}_8$ . Thus, the observed ESR modes are not due to the Walker modes. The ESR signals  $B$  disappear in the field region between  $H_a$  and  $H_s$ . In the field-induced ferromagnetic phase above  $H_s$ , the ESR modes  $B$ ,  $L$ , and  $Q$  show linear field dependence with almost the same slope. Beyond the ESR modes  $B$ ,  $L$ , and  $Q$ , other ones  $M$  and  $P$  are observed.

As we mentioned before, it is considered that the gapless spin liquid state is realized in the field region  $H_c < H < H_s$ . Highly unconventional excitations of the  $S = 1/2$  1D Heisenberg antiferromagnet in magnetic fields, which is a representative of the gapless 1D spin liquid, have been known [16, 17]. At zero field, the spinon excitation of this system is gapless at  $q = 0$  and  $\pi$ , but in the presence of applied magnetic field, the excitation spectrum undergoes drastic change. Besides the gapless excitation at  $q = \pi$  and 0, the magnetic field develops the soft modes at incommensurate wave vectors,  $q_c = \pm 2\pi m(H)$  for a transverse

fluctuation and  $\pi \pm 2\pi m(H)$  for a longitudinal one, with  $m(H)$  being the magnetization per spin. These incommensurate soft modes are manifestations of the Tomonaga-Luttinger liquid state, which is believed to be generally realized in the gapless phase of the quantum 1D antiferromagnets [13]. The gapless wave vectors shift continuously as the magnetization increases. When the magnetization corresponds to half of its saturation, the excitation at  $q = \pi/2$  is gapless, and with further increasing field the excitation becomes fully gapful above the saturation field  $H_s$ . These theoretical indications imply that the ESR modes  $B$ ,  $L$ , and  $Q$  come from the excitations at  $q = 0$ ,  $\pi/2$ , and  $\pi$ , respectively. For the spin liquid phase, the dynamical structure factors (DSFs)  $S^{+-}(q, \omega)$  and  $S^{-+}(q, \omega)$  are calculated by exact diagonalization of  $S = 1/2$  1D XXZ Hamiltonian for a 24-sites system as a function of the ground state magnetization. A theoretical expression of the DSF  $S^{+-}(q, \omega)$  is given as follows:

$$S^{+-}(q, \omega) = 2\pi/N \sum_m |\langle m | S_{-q}^+ | 0 \rangle|^2 \delta(\omega - (E_m - E_0)/\hbar), \quad (2)$$

where  $N$  is the total number of the spins,  $E_m$  is the  $m$ th energy, and  $S_{-q}^+$  is the Fourier transform of the raising operator.  $S^{-+}(q, \omega)$  is given by a replacement of  $S_{-q}^+$  in Eq. (2) to  $S_{-q}^-$ , which is the Fourier transform of the lowering operator. The parameters determined by the analysis of the high field magnetization are used. Figure 4 shows the DSFs calculated for a situation at the total magnetization with 1/4 of the saturation. The ESR modes  $B$ ,  $L$ , and  $Q$  agree well with the calculated lowest excitation energies at  $q = 0$ ,  $\pi/2$ , and  $\pi$ , respectively, as shown in Fig. 3. The excitation in the field-induced ferromagnetic phase is a one-spin-flip excitation, and its energy is obtained exactly as given in Ref. [7]. At the saturation field, the energy, calculated with no NNN interaction at  $k = 0$ , is twice that at  $k = \pi/2$ , whereas the observed resonance frequencies at  $H_s$  are 1370 GHz for the  $B$  ( $q = 0$ ) and 840 GHz for the  $L$  ( $q = \pi/2$ ) modes. Better agreements with the experiments are achieved by introducing the NNN interaction. As seen in Fig. 4, the excitation spectrum in the spin liquid state consists of several continua with peaks. This is because several kinds of spin-flip processes, such as creation or annihilation of the domain wall pair, contribute to the excitation in the spin liquid state under applied field. The ESR modes  $P$  and  $M$  agree with the energies of the second maximum of the DSFs at  $q = \pi/2$  and  $q = \pi$ , respectively.

Finally, we discuss why the excitations at  $q = \pi/2$  and  $q = \pi$ , which are normally unobservable in the ESR measurement, are observed in  $\text{BaCo}_2\text{V}_2\text{O}_8$ . In this compound, slightly distorted  $\text{CoO}_6$  octahedra are edge shared around the fourfold screw axis along the  $c$  direction, forming the peculiar four-step periodical chains. Local coordinates of the  $\text{CoO}_6$  octahedra as well as the nearest-neighbor Co-Co bonds are equivalent for all Co sites. The apical directions of  $\text{CoO}_6$  octahedra, however, are slightly inclined from the

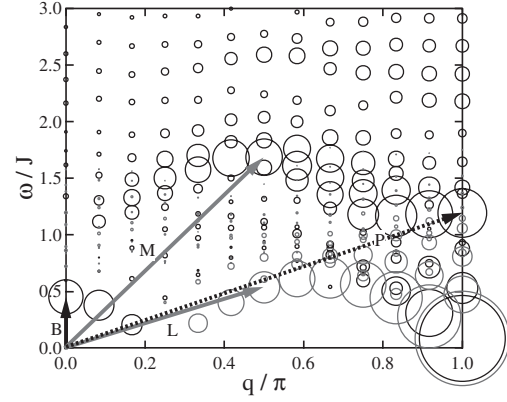


FIG. 4. Dynamical structure factor (DSF) calculated by the exact diagonalization for a situation at the total magnetization with 1/4 of the saturation. Gray circles and black circles represent  $S^{+-}(q, \omega)$  and  $S^{-+}(q, \omega)$ , respectively. Size of the circle corresponds to a magnitude of the DSF.

$c$  axis. Therefore, the magnetic principle axes for each Co site change those directions with a 4-step periodicity along the chain. We speculate that this brings some additional 4-step periodical interaction. Such a periodical interaction will cause a mixing between the magnetic states with  $q = 0$  and  $q = \pi/2$  or  $q = \pi$ , giving rise to finite transition probabilities for the excitations at  $q = \pi/2$  and  $q = \pi$ , and also to the small anomaly in the magnetization at  $H_a$ .

S. K. is grateful to Professor H. Shiba for valuable suggestions about the  $S = 1/2$  1D XXZ model. This work was partly supported by Grant-in-Aid for Science Research from the Japanese Ministry of Education, Science, Sports, Culture and Technology (No. 17072005, No. 18740183, and No. 1870230).

- 
- [1] A. Oosawa *et al.*, J. Phys. Condens. Matter **11**, 265 (1999).
  - [2] T. Nikuni *et al.*, Phys. Rev. Lett. **84**, 5868 (2000).
  - [3] Z. He *et al.*, Phys. Rev. B **72**, 172403 (2005).
  - [4] R. Wichmann and Hk. Muller-Buschbaum, Z. Anorg. Allg. Chem. **534**, 153 (1986).
  - [5] N. Ishimura and H. Shiba, Prog. Theor. Phys. **63**, 743 (1980).
  - [6] K. Amaya *et al.*, J. Phys. Soc. Jpn. **59**, 1810 (1990).
  - [7] H. Shiba *et al.*, J. Phys. Soc. Jpn. **72**, 2326 (2003).
  - [8] S. Kimura *et al.*, in *Yamada Conference LX on Research in High Magnetic Fields, Sendai, Japan, 2006*, J. Phys. Conf. Ser. Vol. 51 (Institute of Physics, London, 2006), p. 99.
  - [9] A. Abragam and M. H. L. Pryce, Proc. R. Soc. A **206**, 173 (1951).
  - [10] M. E. Lines, Phys. Rev. **131**, 546 (1963).
  - [11] L. R. Walker, Phys. Rev. **116**, 1089 (1959).
  - [12] G. Gómez-Santos, Phys. Rev. B **41**, 6788 (1990).
  - [13] F. D. M. Haldane, Phys. Rev. Lett. **45**, 1358 (1980).
  - [14] N. M. Bogoliubov *et al.*, Nucl. Phys. **B275**, 687 (1986).
  - [15] H. Shiba, Prog. Theor. Phys. **64**, 466 (1980).
  - [16] N. Ishimura and H. Shiba, Prog. Theor. Phys. **57**, 1862 (1977).
  - [17] G. Muller *et al.*, Phys. Rev. B **24**, 1429 (1981).